Pergamon

Acta mater. 48 (2000) 4599–4608

Acta MATERIALIA

www.elsevier.com/locate/actamat

ROLE OF THE GRAIN-BOUNDARY PHASE ON THE ELEVATED-TEMPERATURE STRENGTH, TOUGHNESS, FATIGUE AND CREEP RESISTANCE OF SILICON CARBIDE SINTERED WITH Al, B AND C

D. CHEN, M. E. SIXTA, X. F. ZHANG, L. C. DE JONGHE and R. O. RITCHIE*

Materials Sciences Division, Lawrence Berkeley National Laboratory, and Department of Materials Science and Engineering, University of California, Berkeley, CA 94720, USA

Abstract—The high-temperature mechanical properties, specifically strength, fracture toughness, cyclic fatigue-crack growth and creep behavior, of an *in situ* toughened silicon carbide, with Al, B and C sintering additives (ABC-SiC), have been examined at temperatures from ambient to 1500°C with the objective of characterizing the role of the grain-boundary film/phase. It was found that the high strength, cyclic fatigue resistance and particularly the fracture toughness displayed by ABC-SiC at ambient temperatures was not severely compromised at elevated temperatures; indeed, the fatigue-crack growth properties up to 1300°C were essentially identical to those at 25°C, whereas resistance to creep deformation was superior to published results on silicon nitride ceramics. Mechanistically, the damage and shielding mechanisms governing cyclic fatigue-crack advance were essentially unchanged between ~25°C and 1300°C, involving a mutual competition between intergranular cracking ahead of the crack tip and interlocking grain bridging in the crack wake. Moreover, creep deformation was not apparent below ~1400°C, and involved grain-boundary sliding accommodated by diffusion along the interfaces between the grain-boundary film and SiC grains, with little evidence of cavitation. Such unusually good high-temperature properties in ABC-SiC are attributed to crystallization of the grain-boundary amorphous phase, which can occur either *in situ*, due to the prolonged thermal exposure associated with high-temperature fatigue and creep tests, or by prior heat treatment. Moreover, the presence of the crystallized grain-boundary phase did not degrade subsequent ambient-temperature mechanical properties; in fact, the strength, toughness and fatigue properties at 25°C were increased slightly. *© 2000 Acta Metallurgica Inc. Published by Elsevier Science Ltd. All rights reserved.*

Keywords: Ceramics; Fatigue; Creep; Strength; Toughness; High temperature

1. INTRODUCTION

As a high-temperature structural material, silicon carbide (SiC) ceramics offer many advantages, including high melting temperatures, low density, high elastic modulus and strength, and good resistance to creep, oxidation and wear. This combination of properties makes SiC a promising candidate for use in such applications as gas turbines, piston engines and heat exchangers [1, 2], where load-bearing components are required to be subjected to temperatures up to 1500°C for extended periods of time; however, its application to date has been severely limited by its poor fracture toughness properties.

The low inherent fracture toughness of conventional SiC ceramics (K_c is typically ~2–3 MPa $m^{1/2}$) can be improved by several processing and reinforcement routes. One approach is to produce a composite, typically accomplished by incorporating continuous fibers, whiskers or platelets, or second-phase particles [3]. Critical to composites, besides the high fabrication costs, is tailoring the matrix/second-phase interface to be weak enough to provide pull-out without sacrificing strength of the material; moreover, this interface integrity must be maintained at elevated temperatures. For monolithic ceramics, *in situ* toughening can also be effective, as has been demonstrated in the silicon nitride (Si_3N_4) system (e.g., [4]).

Using the latter approach to achieve high toughness in these inherently brittle materials, grains are purposely elongated by processing in the presence of a liquid phase. This results in a microstructure consisting of grains covered with a residual glassy film, with pockets of glass at multiple-grain junctions. Toughness values greater than 10 MPa $m^{1/2}$ have been achieved for Si_3N_4 processed in this fashion; such high toughnesses are generally attributed to intergranular fracture and resulting elastic bridging and

---

* To whom all correspondence should be addressed. Tel.: 001 510 486 5798; fax: 001 510 486 4995.
E-mail address: roritchie@lbl.gov (R.O. Ritchie)

PII: S1359-6454(00)00246-9

frictional pull-out as the interlocking grains separate [4]. The problem for monolithic ceramics is that although the glassy grain-boundary film is considered to be critical in inducing good low-temperature toughness, its presence typically limits properties at high temperatures, such as oxidation, creep resistance and strength.

The origin of the glassy film is associated with the presence of sintering additives. Due to the nature of the bonding, as well as vapor pressures, surface and grain-boundary characteristics make densification in ceramic systems difficult without such additions. These additives promote mass transport either in the solid state or by a liquid-phase formation. While many have been employed in processing SiC, the most common are B and C [5], Al_2O_3 [6], Al_2O_3 and Y_2O_3 [7]. However, in an attempt to avoid the trade-off between low-temperature toughness and high-temperature strength, recent research has focused on a monolithic SiC which is hot-pressed with additions of Al metal as well as B and C. This material, which has been termed ABC-SiC, has been shown to have an ambient-temperature fracture toughness as high as 9 MPa $m^{1/2}$ with strengths of ~650 MPa [8], mechanical properties that are among the highest reported for SiC. The high toughness, which should be compared with that of a commercial SiC (~2.5 MPa $m^{1/2}$), has been attributed to various crack-bridging processes in the crack wake resulting from the intergranular crack path [9]; specifically, crack-tip shielding from both elastic bridging and frictional pull-out of the grains provides a major contribution, with the frictional pull-out component likely to be the most potent.

In situ toughening in SiC results from the large, elongated, plate-like grains that are brought about by exploiting the β-SiC (cubic) to α-SiC (hexagonal) phase transformation. This is akin to the mechanisms in the Si_3N_4 system where acicular, needle-like, grains are obtained under appropriate processing conditions [10]. The microstructure of ABC-SiC consists of such elongated grains with an aspect ratio of *ca*. 3 to 7. These plate-like grains exhibit an interlocking network, and are surrounded (in the as-processed state) by a thin (~1 nm) amorphous grain-boundary film that promotes intergranular fracture; strips of crystalline phases, identified as $Al_8B_4C_7$, Al_4O_4C and Al_2O_3, are also present at grain-boundary triple points.

The sintering additives function in several capacities in *in situ* toughened SiC ceramics. In addition to promoting densification, they also accelerate the β (cubic) to α (hexagonal) phase transformation at temperatures below 1800°C. Several other additive systems, including Al_2O_3 [6] and yttrium aluminum garnet (YAG), also lead to an improved resistance to fracture in SiC; however, these have not as yet resulted in a ceramic with a toughness as high as that of ABC-SiC [7, 11, 12].

The sintering additives in SiC and Si_3N_4 are effective densification aids, but the liquid tends to remain as glassy phases at grain boundaries and multiple-grain junctions [13, 14], degrading the high-temperature properties. Strength degradation in Si_3N_4 is generally attributed to softening of the grain-boundary phase [15]. Similarly, the creep rates of ceramics possessing a glassy grain-boundary phase are degraded compared with the inherent creep resistance [16]. The presence of impurities, introduced as sintering additives, often also reduces the oxidation resistance of Si_3N_4 and SiC [17].

Since the deleterious effects of the grain-boundary and secondary phases on the high-temperature properties are well documented, several approaches have been employed to improve creep and strength without compromising the fracture toughness. These include: (1) crystallization of the grain-boundary phase [18, 19], (2) changing the chemistry of the secondary phase [20], and (3) reducing the amount of sintering additives to minimize the volume of glass present in the final microstructure [21]. The most important parameter governing several of the high-temperature properties is the viscosity of the grain-boundary film. By increasing the viscosity, either by crystallization or by altering the additives to produce a more refractory phase, the high-temperature properties, particularly creep and fracture strength, can be significantly enhanced.

In the present work, we examine the first of these strategies, i.e., specifically how the elevated-temperature mechanical properties of ABC-SiC are affected by the nature of the grain-boundary film/phase, and investigate whether its superior room-temperature strength and toughness properties [8, 9] can be retained at high temperatures. Moreover, due to the contradictory nature [22–32] and paucity of data on creep and especially cyclic fatigue processes in SiC ceramics at such temperatures, not to mention the lack of mechanistic understanding, studies are focused on the characteristics of creep and fatigue-crack propagation behavior from ambient temperatures up to 1500°C.

2. EXPERIMENTAL PROCEDURES

2.1. Material processing

ABC-SiC was processed with submicrometer β-SiC starting powders, which were mixed with additions of 3 wt% Al (as powder with a nominal particle diameter of ~5 μm), 0.6 wt% B (as powder) and 2 wt% C (as Apiezon wax) additions. The calculated value of 2% C was doubled since the carbon yield upon pyrolysis was determined to be ~50%. This carbon source also served as a binder. The Apiezon wax was dissolved in toluene, and the other powders were added; the resulting suspension was agitated ultrasonically for 5–10 min to minimize agglomerate formation, and then stir-dried. The dried material was then ground in a mortar and pestle prior to sieving through a 200 mesh screen.

Hot-pressing was conducted for 1 h at 1900°C, at 50 MPa pressure in a flowing argon atmosphere, in a graphite die using green compacts that were previously formed by uniaxial compression at 35 MPa in a metal die. The resulting hot-pressed disks were surface-ground and polished to a 1 μm diamond powder finish, prior to the machining of samples.

2.2. High-temperature mechanical properties tests

2.2.1. Strength and creep resistance. High-temperature strength and creep tests were performed in four-point bend on 3 mm×3 mm×30 mm beam specimens; testing was conducted with a graphite bend rig in a furnace equipped with tungsten mesh heating elements under a flowing argon atmosphere. Creep experiments were conducted with an initial outer-fiber stress of 100 MPa; the strain was calculated according to the method developed by Hollenberg *et al.* [33]. The stress was fixed for all experiments at temperatures between 1100 and 1500°C. Results were compared with those of various Si_3N_4 ceramics reported in the literature [34–37]. In addition, the effect of prior prolonged exposure to elevated temperatures (annealing) was considered; specifically, the bend strength was evaluated before and after thermal exposures of up to 7 days at 1500°C (in an argon atmosphere).

2.2.2. Fracture toughness and fatigue-crack growth. Fracture toughness (K_c) and cyclic fatigue-crack growth tests were performed on disk-shaped compact-tension DC(T) specimens (28 mm wide, 3 mm thick), containing "large" (>3 mm) through-thickness cracks. Toughness testing was performed on fatigue pre-cracked specimens at temperatures between 25 and 1300°C; in addition, the toughness of as-processed samples was compared with that of samples following a prior thermal exposure for 85 h at 1300°C.

Cyclic fatigue-crack growth testing was performed in general accordance with ASTM Standard E-647. Specifically, DC(T) specimens were cycled at 550, 850, 1200 and 1300°C under automated stress-intensity (K) control while maintaining a constant load ratio (ratio of minimum to maximum applied loads) of $R = 0.1$ at frequencies of $\nu = 3$ and 25 Hz (sinusoidal waveform); corresponding tests at 25°C were carried out under the same conditions only at frequencies of 25 and 1000 Hz. Cyclic fatigue-crack growth rates (da/dN) were monitored as a function of applied strength intensity under decreasing ΔK conditions, with a normalized K-gradient ($1/K \cdot dK/da$) set to -0.08 mm^{-1}. Limited crack-growth measurements were also performed under sustained loading (static fatigue/creep) at 1300°C, with the stress intensity held at the same K_{max} level used in the cyclic tests.

All toughness and crack-growth experiments were conducted on computer-controlled servo-hydraulic mechanical testing machines. Elevated-temperature tests were performed in an environmental chamber/furnace with graphite elements that maintain temperature to within ±1°C. The test environment at elevated temperatures was flowing gaseous argon at atmospheric pressure; corresponding tests at 25°C were conducted in room air. Crack lengths were continuously monitored *in situ* at elevated temperatures by a direct-current electrical-potential drop technique. Use of this technique was made possible by the electrical conductivity of SiC at elevated temperatures; the resistivity of SiC is ~10 Ω cm above 600°C. Details of this method and other experimental procedures are given in Refs. [38] and [39].

2.3. Microstructural characterization

All fracture surfaces and crack profiles were analyzed in a field-emission scanning electron microscope (FESEM). The atomic and structural nature of the grain boundaries was also examined using high-resolution transmission electron microscopy (HRTEM). Chemical compositions of any grain-boundary phases were analyzed by using an X-ray energy-dispersive spectrometer (XEDS) with a 8 nm probe. In addition, the microstructure and damage in regions directly ahead of the crack tip were examined by transmission electron microscopy (TEM). Specifically, 3 mm diameter TEM foils were taken from the crack-tip region of fracture and fatigue test specimens such that the crack line was parallel to the axis of the foil with the crack tip located ~500 μm away from the foil center. The foils, which were ground down to 20 μm using a precision dimpling machine and further thinned by argon-ion milling, were examined on a Philips CM200 microscope, operating at 200 kV.

3. RESULTS AND DISCUSSION

3.1. Microstructure prior to high-temperature testing

The microstructure of as-processed ABC-SiC consisted of a network of interlocking plate-like grains of 5 vol% β-phase (cubic polytype 3C) and 95 vol% α-phase (49 vol% 4H and 46 vol% 6H hexagonal polytypes), with a maximum grain aspect ratio of *ca.* 4 to 5. This grain morphology is quite distinct from that of toughened silicon nitrides, where the grains typically possess high aspect ratios and are acicular, or needle-like, in shape [10]. Between the grains, an amorphous grain-boundary film, typically ~1 nm thick and rich in Al, O and C [40], can be seen in the hot-pressed material (Fig. 1). The remaining sintering additives were found to form bulk secondary phases at triple junctions and multiple-grain junctions; these phases were identified as $Al_4B_7C_8$ and Al_4O_4C [8, 41, 42]. In addition, in specific α-SiC grains, the presence of isolated dislocations could be seen; these dislocations, which were always in very low densities, are likely to be partial dislocations bounding the stacking faults.

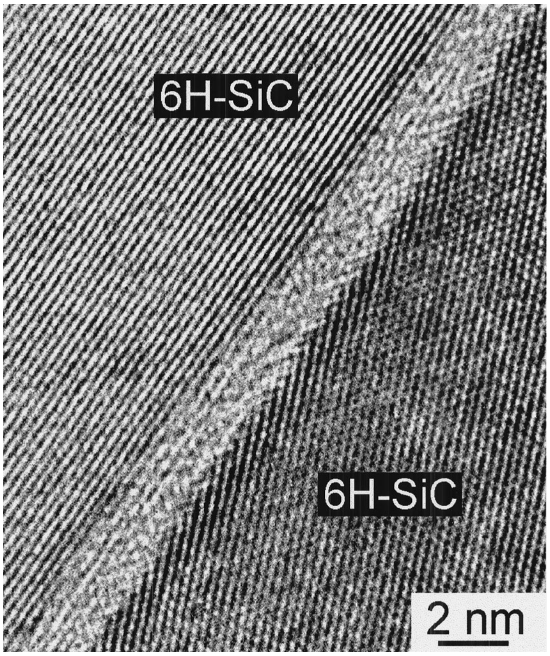

Fig. 1. High-resolution transmission electron micrograph of as-processed ABC-SiC, showing the amorphous grain-boundary film.

3.2. Strength and fracture toughness

The fracture toughness of the as-processed ABC-SiC was measured as $K_c = 6.2$ MPa m$^{1/2}$ at 25°C and 4.3 MPa m$^{1/2}$ at 1300°C. However, annealing for 85 h at 1300°C led to a ~20% increase in toughness over these values, with $K_c = 7.2$ MPa m$^{1/2}$ at 25°C and 5.2 MPa m$^{1/2}$ at 1300°C. Fracture surfaces in all cases were predominantly intergranular.

Corresponding bend strengths were significantly lower at higher temperatures, specifically from ~515 MPa at 25°C to ~100 MPa at 1300°C, with load/displacement plots at both temperatures remaining completely linear. Studies on Si_3N_4 have shown a similar reduction in strength with increasing temperature [14]. However, as with the toughness behavior, in ABC-SiC thermal annealing treatments tended to improve the mechanical properties, in this case quite markedly. Specifically, annealing for 7 days at 1500°C led to a fourfold increase in the bend strength at 1300°C.

HRTEM examination of as-processed bend specimens tested at 1300°C showed that the grain-boundary phase was still fully amorphous (Fig. 1). Thus, whereas the room-temperature strength is governed by the presence of flaws, the fivefold decrease in strength at elevated temperatures can be attributed to the softening of this phase and from grain-boundary sliding [15, 18]. Such observations are consistent with published results on Si_3N_4 with amorphous grain-boundary phases [43].

In contrast, following prolonged high-temperature annealing, where the 1300°C strength increased fourfold, HRTEM imaging indicated that a large majority of the grain-boundary glassy films had become fully crystallized (Fig. 2); this was found to occur at all temperatures above ~1100°C for times in excess of ~5 h. Moreover, the average thickness of grain-boundary film decreased to less than ~1 nm, with a corresponding increase in the Al concentration (revealed by the XEDS spectra [40]). Such crystallization of the grain-boundary phase clearly would minimize softening and grain-boundary sliding and possibly induced flaw healing within this region, which would account for the fourfold increase in strength.

Although crystallization is less common in Si_3N_4, when it does occur it has been found to degrade the subsequent low-temperature strength and toughness [44]. Remarkably, in ABC-SiC the strength at 25°C was increased after the crystallization, as discussed in detail elsewhere [45]. In addition, the toughness at both 25 and 1300°C was increased by some 16 to 21% by prior crystallization, as noted above [46].

Microstructural variations in ceramics often have opposing effects on strength and toughness, e.g., the decrease in strength and increase in toughness with coarser grain sizes in Si_3N_4 and SiC; however, the crystallization of the grain-boundary phase in ABC-SiC acts to promote both strength and toughness, at both low and high temperatures, and (as discussed below) can increase the resistance to cyclic fatigue as well.

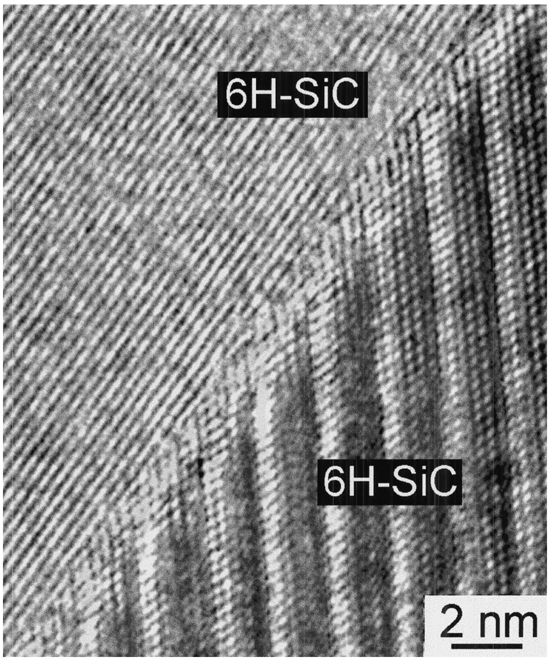

Fig. 2. High-resolution transmission electron micrograph of a grain boundary in ABC-SiC after high-temperature annealing (1400°C/840 h), showing that the amorphous layer has become fully crystallized.

3.3. *Creep behavior*

The creep properties of ABC-SiC between 1100 and 1500°C, in the form of the logarithm of the strain rate, $\log \dot{\varepsilon}$, as a function of reciprocal temperature, $1/T$, are compared in Fig. 3 with bending creep test results for three grades of silicon nitride and SiC with 0.3% Al [34–37]. It can be seen that the creep resistance of ABC-SiC is comparable to, or significantly better than, the creep resistance of these other advanced ceramics. The apparent creep activation energy, Q_a, was calculated to be ~225 kJ/mol at a stress of 100 MPa. In addition, Norton power-law behavior, with a stress exponent of *ca*. 1, was found for tests conducted between 50 and 200 MPa [47].

Although creep rates at 1400°C for ABC-SiC and the best Si_3N_4 [35] were comparable, the lower temperature dependence and activation energy of ABC-SiC meant that it exhibited lower steady-state creep rates than any Si_3N_4 as the temperature was increased to 1500°C. ABC-SiC also exhibited low creep rates at stresses that were a much higher percentage of its fracture strength than the silicon nitrides; for example, the Si_3N_4/SiC nano-composite had a similar creep rate in bending at 1400°C, but with a bend strength of 895 MPa, compared with ~300 MPa for ABC-SiC.

On the microscopic scale, a low density of dislocations with no apparent slip bands could be observed occasionally in isolated grains in ABC-SiC (Fig. 4); the density of these dislocations increased with increasing temperature. Evidence of cavitation, however, was not found after creep (and fatigue) testing at 1300°C (and below). The threshold for creep cavitiation appeared to be around 1400°C, where grain-boundary cavities were observed on the tensile, but not compression, side of the beams (Fig. 5). Cavities were formed both at two-grain and multiple-grain junctions. Even at higher temperatures, while the dislocation density was higher, slip bands were still not a dominant feature. As noted above, the grain-boundary films became fully crystallized during the long holding times at creep temperatures, similar to behavior during pre-annealing and fatigue testing (Fig. 2). Additionally, the concentration of impurities in the boundary film was found to increase slightly compared with the as-hot-pressed material; in addition, the aluminum concentration increased as the creep temperature increased [40].

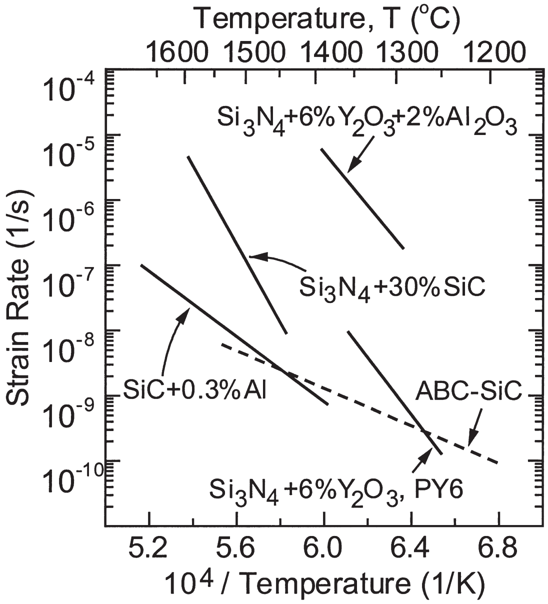

Fig. 3. Comparison of creep rates for ABC-SiC (dashed line) with various silicon-based ceramics (solid lines). All data were collected from bend creep tests at a load of 100 MPa.

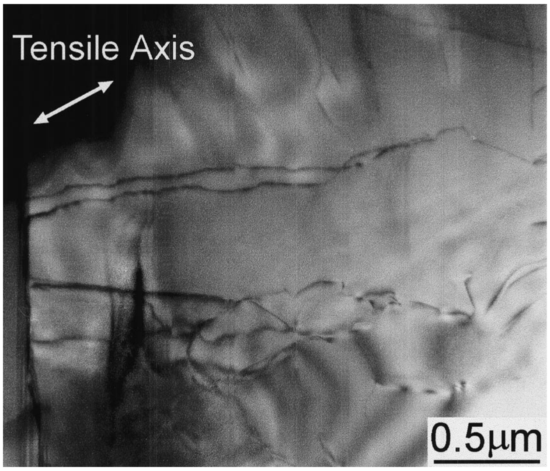

Fig. 4. Transmission electron micrograph of ABC-SiC showing dislocations, located in a residual β-SiC grain, on the tensile edge of a specimen crept at 1200°C for 670 h under a stress of up to 175 MPa.

Evaluation of the stress and temperature dependence, in conjunction with the microstructural changes, indicated that the controlling creep mechanism in ABC-SiC was grain-boundary sliding

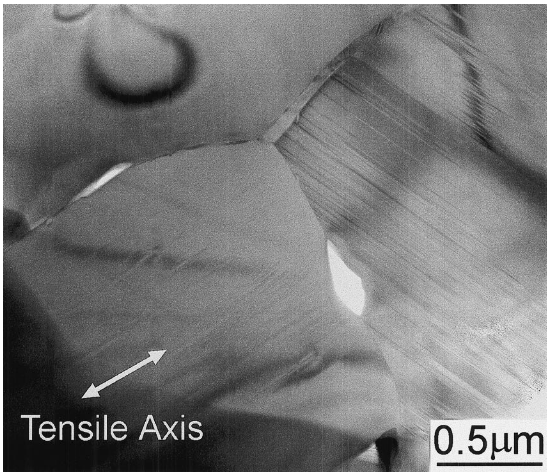

Fig. 5. Transmission electron micrograph of ABC-SiC showing grain-boundary cavities at two-grain junctions on the tensile edge of a specimen crept at 1400°C for 840 h under 200 MPa.

accommodated by diffusion along the grain-boundary film/silicon carbide interface. A parallel mechanism of cavitation was also operative above 1400°C in tensile-loaded regions, but the low density of cavities present and the stress exponent of unity suggest that cavitation was not the dominant component in the creep deformation at the temperatures and total strains examined. Further details on the creep mechanisms in ABC-SiC are reported elsewhere [47].

3.4. Fatigue-crack growth behavior

Figure 6 illustrates the variation in fatigue-crack growth rates, da/dN, with applied stress-intensity range, ΔK, at a load ratio of 0.1 for ABC-SiC under different test conditions, showing the effects of temperature and loading frequency on the cyclic fatigue behavior. It can be seen that at both ambient and elevated temperatures, crack-growth rates display a marked sensitivity to the stress intensity regardless of the loading frequency; this is a common characteristic of monolithic ceramics at low homologous temperatures [48]. In terms of a simple Paris power-law formation:

$$da/dN = C\Delta K^m \tag{1}$$

(where C and m are scaling constants), these data show a Paris exponent m between 35 and 68.

Although changing the cyclic frequency over the range 3 to 1000 Hz had little effect on fatigue-crack growth behavior, growth rates were accelerated with increasing temperature. Indeed, ΔK_{th} fatigue thresholds were decreased from just over 5 MPa m$^{1/2}$ at 25°C to between 3.3 and 3.4 MPa m$^{1/2}$ at 1200°C; interestingly, there was no further decline at 1300°C. Mechanistically, the lack of a frequency effect in ABC-SiC at ambient temperatures is expected as crack advance occurs via predominantly intergranular cracking ahead of the tip, balanced by shielding by grain bridging in the wake, both essentially rate-insensitive processes [49–51]. However, the absence of a frequency effect at elevated temperatures is much more surprising, particularly since comparable materials, such as Si_3N_4, Al_2O_3 and silicide-matrix ceramics, show a marked sensitivity to frequency at temperatures due to the onset of creep damage above ~1000°C [22, 25–27, 52]. As described below, fatigue fracture mechanisms at 850 to 1300°C in the present material were effectively identical to those at room temperature, which is consistent with the absence of significant creep phenomena below 1300°C.

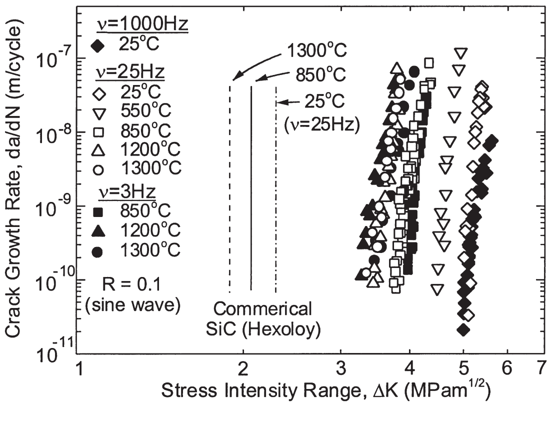

Fig. 6. Cyclic fatigue-crack growth rates, da/dN, in ABC-SiC as a function of the applied stress-intensity range, ΔK, for the tests conducted at temperatures between 25 and 1300°C, load ratio $R = 0.1$, and frequencies between 3 and 1000 Hz. For comparison, the crack-growth behavior of commercial SiC (Hexoloy) is also illustrated.

The fracture toughness and fatigue-crack growth resistance of ABC-SiC were found to be far superior to those of commercial SiC (Hexoloy) at both room and elevated temperatures. Results at 25 to 1300°C, which are compared with ABC-SiC in Fig. 6, indicate that Hexoloy fails catastrophically, with no cycle-dependent cracking, at stress intensities some 40–50% lower than the fatigue thresholds in ABC-SiC. Such extremely brittle behavior is attributed to the absence of toughening from crack bridging behind the crack tip, resulting from its fully transgranular mode of fracture.

A comparison of the crack-growth velocities under cyclic and static (sustained) loading is shown in Fig. 7. It can be seen that at both ambient and elevated temperatures, growth rates in ABC-SiC under cyclic loads were significantly faster than under sustained loading (static fatigue) at equivalent stress-intensity levels. Such behavior has been observed previously in Mg-PSZ [53, 54], Al_2O_3 [55] and Si_3N_4 [56], and

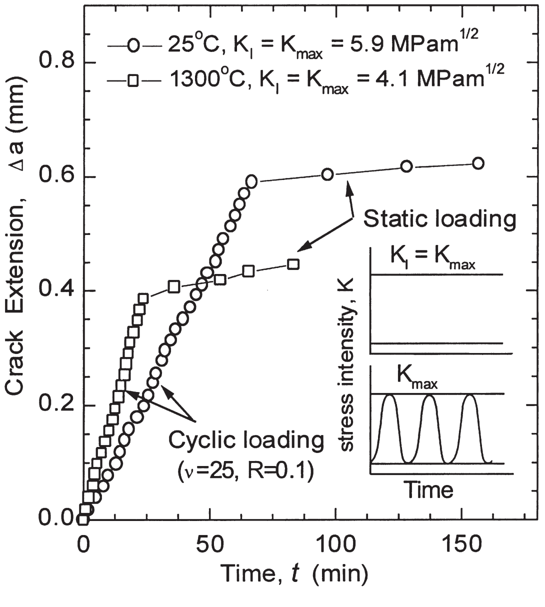

Fig. 7. Crack extension, Δa, plotted as function of time, t, demonstrating the effect of sustained loading versus cyclic loading conditions, at a fixed maximum stress intensity ($K_I = K_{max}$). Plotted is behavior at 25°C, where $K_I = K_{max} = 5.9$ MPa m$^{1/2}$, and at 1300°C, where $K_I = K_{max} = 4.1$ MPa m$^{1/2}$.

is consistent with the fact that at low temperatures, crack-advance (damage) mechanisms are identical under both types of loading; specifically, it is the cyclic-loading-induced degradation in wake shielding that accelerates growth rates under cyclic loads. In contrast, the sustained-load mechanisms at elevated temperatures are generally far more damaging in such ceramics as Al_2O_3 and Si_3N_4 [22, 26–28] because of the onset of creep damage, which can cause softening and cavitation in the grain-boundary films [23]. Such behavior was not seen in ABC-SiC at temperatures up to 1300°C.

Scanning electron microscopy (SEM) of fracture surfaces and crack profiles in ABC-SiC at 1300°C revealed a predominantly intergranular fracture under both static and cyclic loads [Fig. 8(a) and (c)], with extensive interlocking grain bridging behind the crack tip [Fig. 8(b) and (d)]. Also noticeable on the cyclic fatigue surfaces was the presence of debris, formed by wear and abrasion of the bridging crack faces during cycling. Fracture surfaces at 25°C were essentially identical [9], implying that a similar sequence of mechanisms, namely intergranular cracking coupled with degradation of the resulting wake zone of bridging grains, is active at both temperatures.

TEM studies of regions in the immediate vicinity of the crack tip provided direct confirmation of these observations. Akin to behavior at room temperature, crack extension at 1300°C under both sustained and cyclic loading was predominantly along the grain boundaries with no indication of cavitation damage ahead of the tip or viscous-phase bridging in the wake (Fig. 9). HRTEM observations also revealed that the grain-boundary films had fully crystallized (e.g., Fig. 2) *in situ* during the high-temperature fatigue tests, which typically lasted *ca*. 3 to 10 days at 1200°C or 1300°C.

The absence of creep damage and/or viscous softening of the grain-boundary phase at 1300°C in ABC-SiC is quite startling. In Si_3N_4 [24, 25], Al_2O_3 [26] and silicide-matrix composites [52] at these temperatures, cavitation along grain boundaries, microcracking zones and viscous-phase bridging are commonly observed. The unique high-temperature characteristics of ABC-SiC appear to be a result of the *in situ* crystallization of grain-boundary glassy phase.

Even though the primary mechanisms of damage (intergranular cracking) and shielding (grain bridging) are apparently unchanged between 25 and 1300°C in ABC-SiC, there is a small change in the fatigue-crack growth resistance in that fatigue thresholds ΔK_{th} are approximately 30% lower at the higher temperature. This may be rationalized by considering

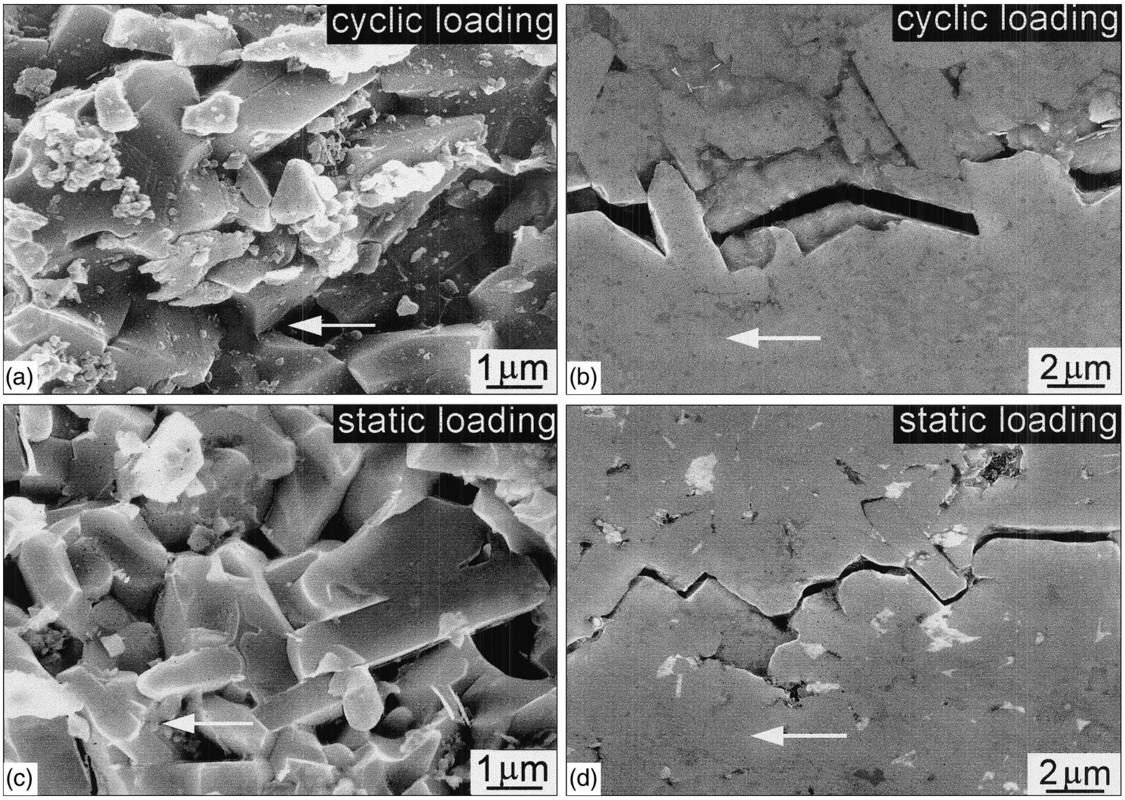

Fig. 8. Scanning electron micrographs of (a, c) fracture surfaces and (b, d) crack trajectories behind the crack tip in ABC-SiC at 1300°C under (a, b) cyclic loading with frequency $\nu = 25$ Hz, load ratio $R = 0.1$ and maximum stress intensity $K_{max} = 4.1$ MPa $m^{1/2}$; and (c, d) static loading with stress-intensity factor $K_I = 4.1$ MPa $m^{1/2}$. Arrows indicate direction of crack propagation.

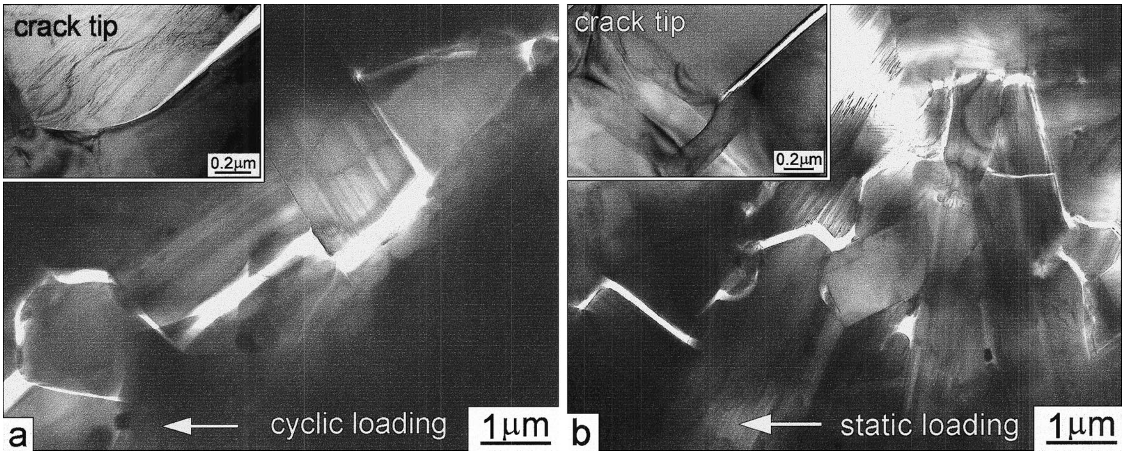

Fig. 9. Transmission electron micrographs of the crack profiles at the crack-tip region in ABC-SiC at 1300°C under (a) cyclic loading ($R = 0.1$, $\nu = 25$ Hz, $K_{max} = 4.1$ MPa $m^{1/2}$) and (b) sustained loading ($K_I = 4.1$ MPa $m^{1/2}$). Arrows indicate the general direction of crack propagation.

the nature of grain bridging [57, 58] and its degradation under cyclic loading due to frictional wear [59, 60]. The pull-out resistance from frictional tractions generated via sliding contact of opposing crack faces [61] is proportional to the normal stress acting on the interface, which in turn is a function of the residual stress resulting from thermal expansion anisotropy during cooling from the processing temperature [57]. As the residual stresses will "anneal out" with increasing temperature, the normal stress will decrease. However, once crystallization of grain-boundary phase occurs above ~1100°C, the frictional coefficient may be expected to be higher. Thus, the minimal change in cyclic fatigue properties between 25 and 1300°C can be related to: (1) the lack of any apparent change in mechanisms, (2) the fact that the decrease in residual stress with temperature is compensated by an increase in the frictional coefficient, and (3) the absence of significant creep damage, the latter two effects being associated with the *in situ* crystallization of the grain-boundary phase. Such a result is consistent with previous studies in other ceramics that show a beneficial effect of crystallization on oxidation and mechanical properties at elevated temperatures [62–65].

4. CONCLUDING REMARKS

Structural ceramics have often been regarded as exhibiting a conflict between toughness, strength and fatigue resistance. Indeed, this conflict is not unlike the competition between brittleness and strength in metallic systems. A summary of many results on creep and toughness at 1300°C for SiC and Si_3N_4, extracted from the literature, is shown in Fig. 10 to illustrate this paradigm, and to show that ABC-SiC can be processed to negate it. Essential in the success of retaining simultaneously strength, toughness and fatigue and creep resistance, is the creation of a crystalline grain-boundary film that retains a stable structure and composition up to high temperatures. In ABC-SiC, this can be achieved *in situ* at elevated temperatures, or by a high-temperature annealing process. Whereas high-temperature post-processing treatments of this kind are relatively uncommon for enhancing the properties of ceramics, their value is evident here. It should be added that the beneficial effects of the Al, B and C additives and the subsequent heat treatments could not, at this time, have been predicted from either first-principles computations or existing lore, but rather resulted from extensive experimentation and application of general materials science principles. It is hoped that, in the future, computational efforts may assist in further developing the necessary nature and role of the grain-boundary films, to improve further the mechanical behavior of these high-temperature structural ceramics.

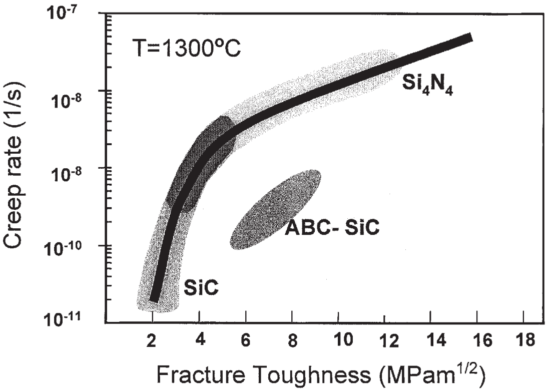

Fig. 10. Summary of literature data on simultaneous creep and toughness values for SiC and Si_3N_4 at 1300°C. ABC-SiC can be processed to be significantly better than the general trend.

5. SUMMARY AND CONCLUSIONS

The high-temperature mechanical properties, including strength, fracture toughness, creep and cyclic fatigue properties, of an *in situ* toughened silicon carbide sintered with Al, B and C (ABC-SiC) have been studied, and related to the corresponding microstructural and mechanistic characteristics. Based on this work, the following conclusions can be made.

1. High-temperature annealing at 1100 to 1500°C was found to lead to a remarkable improvement in mechanical properties. For example, although the bend strength of as-processed ABC-SiC was decreased from ~515 to ~100 MPa with increase in temperature from 25 to 1300°C, prior annealing for 7 days at 1500°C resulted in a factor of four increase in strength at 1300°C. Similarly, the ~30% decrease in fracture toughness between 25 and 1300°C was partially offset by prior annealing for 85 h at 1300°C, which produced a ~20% increase of toughness at both 25 and 1300°C. Such annealing treatments were found to result in full crystallization of the glassy grain-boundary phase.
2. The creep resistance of ABC-SiC was found to be comparable to, or better than, that of most silicon nitrides reported in the literature. Moreover, it displayed a much lower temperature dependence of steady-state creep rates with a creep activation energy of ~225 kJ/mol at an applied stress of 100 MPa. Using a Norton power law to characterize creep rates, the stress exponent was found to be approximately unity for applied stresses between 50 and 200 MPa.
3. Mechanistically, dislocations (but not slip bands) were seen in creep specimens in isolated grains, with a density that increased with increasing temperature. However, extensive creep damage in the form of grain-boundary cavitation was not seen at any temperature below 1400°C; isolated cavities were observed above 1400°C at two-grain and multiple-grain junctions, but only on the tensile side of the creeping beams.
4. Based on these observations, the controlling creep mechanism in ABC-SiC was reasoned to be grain-boundary sliding accommodated by diffusion along the grain-boundary film/SiC interface; cavitation was not found to play a significant role in creep deformation at temperatures up to 1500°C.
5. Cyclic fatigue-crack growth rates in ABC-SiC were only minimally increased, and ΔK_{th} thresholds decreased by ~30%, with increase in temperature from 25 to 1300°C; behavior, however, was independent of frequency. At equivalent stress-intensity levels, crack-growth velocities under cyclic loads were significantly faster than those under static loads at both 25 and 1300°C. The fatigue-crack growth resistance of ABC-SiC was found to be superior to that of commercial SiC (Hexoloy) at all temperatures tested.
6. Crack profile and fractographic studies showed a predominantly intergranular cracking mode at both low and high temperatures, with crack-tip shielding by grain bridging in the crack wake. Such bridging was degraded under cyclic loads, as evidenced by the extensive wear debris on fatigue fracture surfaces. No evidence of creep cavitation or any form of viscous-ligament bridging by the grain-boundary glassy phase was seen at all temperatures up to 1300°C. The mechanistic sequence of intergranular damage ahead of the crack tip, and the cyclic-loading-induced degradation of grain bridging behind the tip, was considered to be essentially unchanged between 25 and 1300°C.
7. HRTEM observations revealed that the grain-boundary film/phase in specimens which underwent high-temperature (≥1100°C) fatigue/creep tests or prior annealing treatments were all fully crystallized. Such crystallized grain boundaries are considered to be the primary reason for the impressive mechanical properties of ABC-SiC at elevated temperatures, involving simultaneous enhancements in high-temperature strength, toughness, fatigue and creep resistance.

Acknowledgements—This work was supported by the Director, Office of Science, Office of Basic Energy Sciences, Materials Sciences Division of the US Department of Energy under Contract No. DE-AC03-76SF00098. Particular thanks are due to Drs J. M. McNaney and C. J. Gilbert for helpful discussions and experimental assistance.

REFERENCES

1. Helms, H. E. and Haley, P. J. in *Third International Symposium on Ceramic Materials and Components for Engines*, ed. V. J. Tennery, American Ceramic Society, Westerville, OH, 1989, p. 1347.
2. Jacobson, N. S. *J. Am. Ceram. Soc.*, 1993, **76**, 3.
3. Evans, A. G. *J. Am. Ceram. Soc.*, 1990, **73**, 187.
4. Becher, P. F. *J. Am. Ceram. Soc.*, 1991, **74**, 255.
5. Prochazka, S. and Scanlan, R. M. *J. Am. Ceram. Soc.*, 1975, **58**, 72.
6. Mulla, M. A. and Krstic, V. D. *Ceram. Bull.*, 1991, **7**, 439.
7. Kim, D. -H. and Kim, C. H. *J. Am. Ceram. Soc.*, 1990, **73**, 1431.
8. Cao, J. J., MoberlyChan, W. J., De Jonghe, L. C., Gilbert, C. J. and Ritchie, R. O. *J. Am. Ceram. Soc.*, 1996, **79**, 461.
9. Gilbert, C. J., Cao, J. J., MoberlyChan, W. J., De Jonghe, L. C. and Ritchie, R. O. *Acta mater.*, 1996, **44**, 3199.
10. Menon, M. N., Fang, H. T., Wu, D. C., Jenkins, M. G., Ferber, M. K., More, K. L., Hubbard, C. R. and Nolan, T. A. *J. Am. Ceram. Soc.*, 1994, **77**, 1217.
11. Lee, S. K. and Kim, C. H. *J. Am. Ceram. Soc.*, 1994, **77**, 1655.
12. Padture, N. P. *J. Am. Ceram. Soc.*, 1994, **77**, 519.
13. Clarke, D. R. and Thomas, G. *J. Am. Ceram. Soc.*, 1977, **60**, 491.
14. Ferber, M. K. and Jenkins, M. G. *J. Am. Ceram. Soc.*, 1992, **75**, 2453.
15. Lloyd, D. E. in *Special Ceramics 4*, ed. P. Popper, British Ceramics Research Association, Stoke-on-Trent, 1968, p. 165.
16. Davis, R. F. and Carter, C. H. Jr. in *Advanced Ceramics*, ed. S. Saito, Oxford University Press, New York, NY, 1988, p. 95.
17. Singhal, S. C. and Lange, F. F. *J. Am. Ceram. Soc.*, 1975, **58**, 433.
18. Tsuge, A., Nishida, K. and Komatsu, M. *J. Am. Ceram. Soc.*, 1975, **58**, 323.
19. Clarke, D. R., Lange, F. F. and Schnittgrund, G. D. *J. Am. Ceram. Soc.*, 1982, **65**, C51.

20. Wiederhorn, S. M., Fields, B. A. and Hockey, B. J. *Mater. Sci. Eng. A*, 1994, **A176**, 51.
21. Park, H., Kim, H. -E. and Niihara, K. *J. Am. Ceram. Soc.*, 1997, **80**, 750.
22. Hansson, T., Miyashita, Y. and Mutoh, Y. in *Fracture Mechanics of Ceramics*, Vol. 12, ed. R. C. Bradt. Plenum Press, New York, 1996, p. 187.
23. Lin, C. -K. J. and Socie, D. F. *J. Am. Ceram. Soc.*, 1991, **74**, 1511.
24. Ramamurty, U., Hansson, T. and Suresh, S. *J. Am. Ceram. Soc.*, 1994, **77**, 2985.
25. Zhang, Y. H. and Edwards, L. *Mater. Sci. Eng. A*, 1998, **A256**, 144.
26. Ewart, L. and Suresh, S. *J. Mater. Sci.*, 1992, **27**, 5181.
27. Liu, S. -Y., Chen, I. -W. and Tien, T. -Y. *J. Am. Ceram. Soc.*, 1994, **77**, 137.
28. Lin, C. -K. J., Jenkins, M. G. and Ferber, M. K. *J. Mater. Sci.*, 1994, **29**, 3517.
29. Jenkins, M. G., Ferber, M. K. and Lin, C. K. J. *J. Am. Ceram. Soc.*, 1993, **76**, 788.
30. Liu, S. -Y. and Chen, I. -W. *Acta mater.*, 1996, **44**, 2079.
31. Evans, A. G., Russel, L. R. and Richerson, D. W. *Metall. Trans.*, 1975, **6A**, 707.
32. Blumenthal, W. and Evans, A. G. *J. Am. Ceram. Soc.*, 1984, **67**, 751.
33. Hollenberg, G. W., Terwilliger, G. R. and Gordon, R. S. *J. Am. Ceram. Soc.*, 1971, **54**, 196.
34. Rendtel, A. and Hübner, H. *J. Am. Ceram. Soc.*, 1998, **81**, 1109.
35. Todd, J. A. and Xu, Z. Y. *J. Mater. Sci.*, 1989, **24**, 4443.
36. Chermant, J. L. and Osterstock, F. *Mater. Sci. Eng.*, 1985, **71**, 147.
37. Ferber, M. K. and Jenkins, G. *J. Am. Ceram. Soc.*, 1992, **75**, 2453.
38. Chen, D., Gilbert, C. J., Zhang, X. F. and Ritchie, R. O. *Acta mater.*, 2000, **48**, 659.
39. Chen, D., Gilbert, C. J. and Ritchie, R. O., *J. Test. Eval.*, 2000, **28**, 236.
40. Zhang, X. F., Sixta, M. E. and De Jonghe, L. C., *J. Am. Ceram. Soc.*, 2000, in press.
41. MoberlyChan, W. J., Cao, J. J., Niu, M. Y. and De Jonghe, L. C. in *High Performance Composites, TMS Conference Proceedings*, ed. K. K. Chawla, P. K. Liaw and S. G. Fishman, Minerals, Metals and Materials Society, Warrrendale, PA, 1994, p. 219.
42. Mitchell, T. D., De Jonghe, L. C., MoberlyChan, W. J. and Ritchie, R. O. *J. Am. Ceram. Soc.*, 1995, **78**, 97.
43. Huang, Z. -K., Rosenflanz, A. and Chen, I. -W. *J. Am. Ceram. Soc.*, 1997, **80**, 1256.
44. Nishimura, T., Mitomo, M. and Suematsu, H. *J. Mater. Res.*, 1997, **12**, 203.
45. Sixta, M. E., Zhang, X. F. and De Jonghe, L. C., *J. Am. Ceram. Soc.*, 2000, **83**, in press.
46. Chen, D., Gilbert, C. J., Zhang, X. F. and Ritchie, R. O., *J. Am. Ceram. Soc.*, 2000, **83**, in press.
47. Sixta, M. E., Zhang, X. F. and De Jonghe, L. C., *J. Am. Ceram. Soc.*, 2000, submitted for publication.
48. Ritchie, R. O. and Dauskardt, R. H. *J. Ceram. Soc. Jpn.*, 1991, **99**, 1047.
49. Guiu, F., Li, M. and Reece, M. *J. Am. Ceram. Soc.*, 1992, **75**, 2976.
50. Kishimoto, H., Ueno, A. and Okawara, S. *J. Am. Ceram. Soc.*, 1994, **77**, 1324.
51. Li, M. and Guiu, F. *Acta metall. mater.*, 1995, **43**, 1871.
52. Ramamurty, U., Kim, A. S. and Suresh, S. *J. Am. Ceram. Soc.*, 1993, **76**, 1953.
53. Dauskardt, R. H., Yu, W. and Ritchie, R. O. *J. Am. Ceram. Soc.*, 1987, **70**, C248.
54. Dauskardt, R. H., Marshall, D. B. and Ritchie, R. O. *J. Am. Ceram. Soc.*, 1990, **73**, 893.
55. Gilbert, C. J., Dauskardt, D. R., Steinbrech, R. W., Petrany, R. N. and Ritchie, R. O. *J. Mater. Sci.*, 1995, **30**, 643.
56. Gilbert, C. J., Dauskardt, R. H. and Ritchie, R. O. *J. Am. Ceram. Soc.*, 1995, **78**, 2291.
57. Foote, R. M. L., Mai, Y. -W. and Cotterell, B. *J. Mech. Phys. Solids*, 1986, **34**, 593.
58. Lawn, B. R. *Fracture of Brittle Solids*, 2nd ed. Cambridge University Press, New York, 1993.
59. Lathabai, S., Rödel, J. and Lawn, B. *J. Am. Ceram. Soc.*, 1991, **74**, 1340.
60. Dauskardt, R. H. *Acta metall. mater.*, 1993, **41**, 2765.
61. Swanson, P. L., Fairbanks, C. J., Lawn, B. R., Mai, Y. -W. and Hockey, B. J. *J. Am. Ceram. Soc.*, 1987, **70**, 279.
62. Lange, F. F., Davis, B. I. and Metcalf, M. G. *J. Mater. Sci.*, 1983, **18**, 1497.
63. Cinibulk, M. K., Thomas, G. and Johnson, S. M. *J. Am. Ceram. Soc.*, 1992, **75**, 2037.
64. Cinibulk, M. K., Thomas, G. and Johnson, S. M. *J. Am. Ceram. Soc.*, 1992, **75**, 2044.
65. Becker, P. F., Hwang, S. L. and Hsueh, C. H. *MRS Bull.*, 1995, **20**, 23.